ELSEVIER

Tectonophysics 288 (1998) 237–250

TECTONOPHYSICS

Structural insight into the south Ryukyu margin: effects of the subducting Gagua Ridge

Philippe Schnürle [a,*], Char-Shine Liu [a], Serge E. Lallemand [b], Donald L. Reed [c]

[a] *Institute of Oceanography, National Taiwan University, Taipei, Taiwan*
[b] *Laboratoire de Géophysique et Tectonique, Université de Montpellier II, 34095, Montpellier Cedex 05, France*
[c] *Department of Geology, San Jose State University, San Jose, CA 95192, USA*

Accepted 19 November 1997

Abstract

This study presents three multi-channel deep seismic reflection profiles located in the south Ryukyu margin between 122°30'E and 123°30'E, where a N–S-trending oceanic ridge, the Gagua Ridge, is entering the subduction zone, for the purpose of examining the effects of ridge subduction on structures of the forearc region. Structural features which correspond to different stages of the oblique ridge subduction are observed. East of 123°E, a short-lived sequence of indentation, tunneling, then resumption of frontal accretion occurred in the accretionary wedge (the Yaeyama Ridge) as the subducted portion of the Gagua Ridge swept the overriding Ryukyu margin from below along the northwesterly convergent direction. Under the forearc basin, the subducted portion of the Gagua Ridge is uplifting the arc basement to form the Nanao Basement Rise which separates the sedimentary strata of the Nanao and East Nanao forearc basins. Results from this study suggest that the oblique subduction of the Gagua Ridge has not only affected accretionary wedge structures but also the arc basement of the south Ryukyu margin.

Keywords: Ryukyu Trench; West Philippine Basin; Gagua Ridge subduction; Taiwan

1. Introduction

The Ryukyu margin forms the northwestern boundary of the Philippine Sea plate and the Chinese continental margin (Fig. 1). The Ryukyu Island Arc extends over 1200 km between Kyushu (Japan) and Taiwan. Along the Ryukyu Trench, the subduction has been active since the Late Cretaceous (Le Pichon et al., 1985). At its southwestern extremity, the Ryukyu subduction zone terminates in the Taiwan collision zone. The geology of the southern Ryukyu Islands is characterized by high-pressure metamorphic rocks, Eocene volcanics and limestone, and Lower Miocene sediments (Kizaki, 1986), while the island of Taiwan was formed during the collision of the Luzon volcanic arc and the Chinese passive margin in the last 5 million years (e.g. Ho, 1986; Teng, 1990). The present plate boundary between the Eurasia and the Philippine Sea plates passes from the Manila Trench, south of Taiwan, to the Ryukyu Trench, east of Taiwan, through the Taiwan mountain belt. Within this collision zone, thrusts are accommodating the shortening between the two plates at a rate of 7.1 cm/yr in a direction of N308° (Seno et al., 1993).

* Corresponding author. Fax: 886 2 362 6092.

0040-1951/98/$19.00
PII S0040-1951(97)00298-9

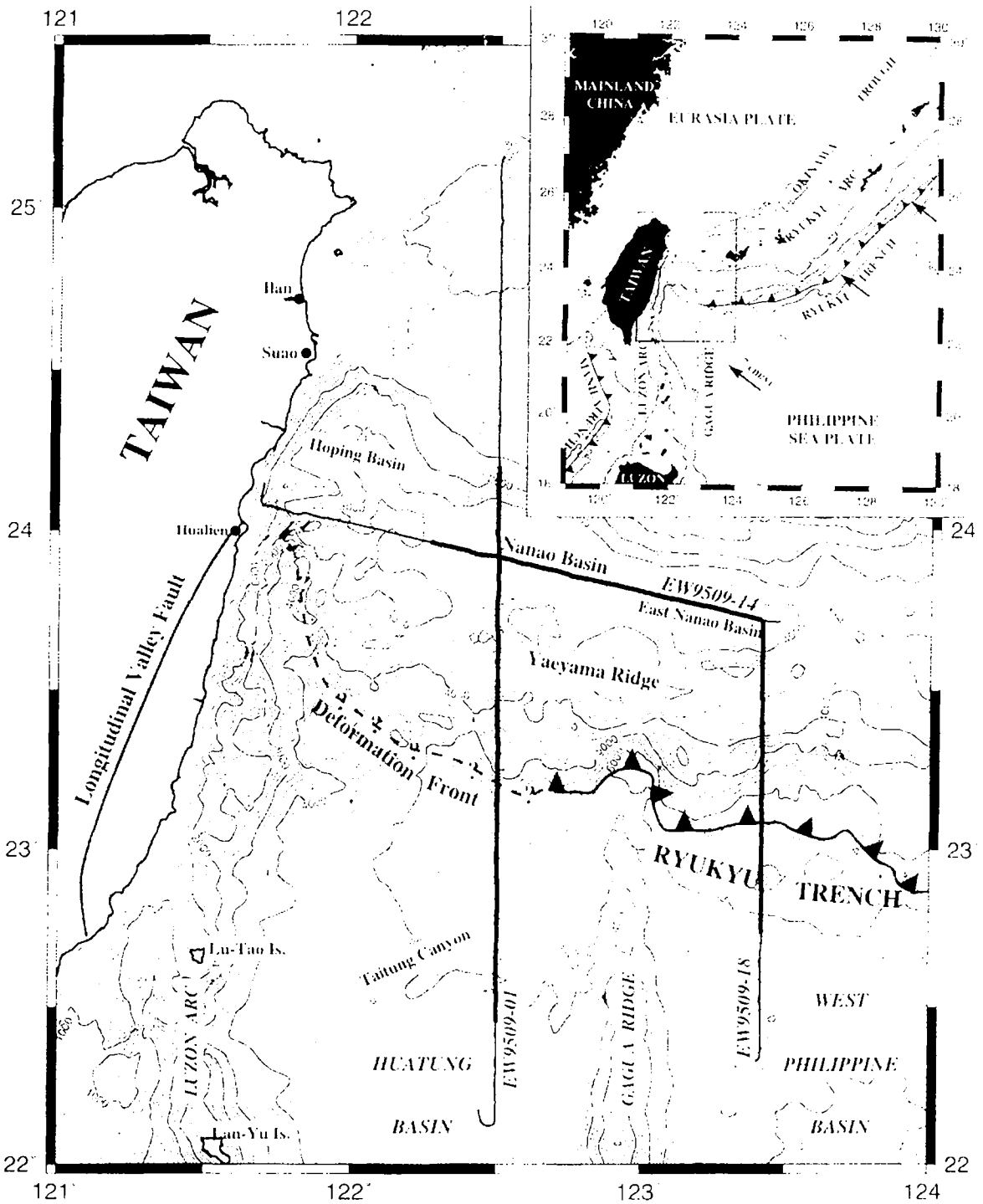

Fig. 1. Bathymetric map of the southern Ryukyu arc–trench system at the vicinity of the Gagua Ridge (after Liu et al., 1996b). Isobaths are in 500 m. Location of the TAICRUST multi-channel seismic profiles EW9509-1 (profile 1), EW9509-18 (profile 2), and EW9509-14 (profile 3) are given. Thick lines indicate the portion of the seismic profiles shown in Figs. 2, 5 and 6. Inset shows the geodynamic framework of the Philippine Sea–Eurasia plate boundary. Isobaths are in 1000-m contours. Relative convergence vectors are after Seno et al. (1993). Map is generated using GMT (Wessel and Smith, 1995).

Offshore east Taiwan, a 40–60-km-wide accretionary wedge, the Yaeyama Ridge, forms the toe of the convergent Ryukyu margin. A series of 30–40-km-wide forearc basins were formed between the growing Yaeyama Ridge and the southern flank of the Ryukyu Arc basement (Fig. 1). Typical convergent structures of the Ryukyu margin extend westward to about 122°30′E (Liu et al., 1996a). Further west, the deformation front connects the western end of the Ryukyu Trench at 23°N to the northern end of the Longitudinal Valley fault near the east coast of Taiwan at 24°N. Along this northward-bending deformation front, relative convergence is extremely oblique (Fig. 1). Frontal accretion is not active in this portion of the accretionary wedge (Lallemand et al., 1997), and NW–SE-trending strike-slip faults are observed in the accretionary wedge (Liu et al., 1996a).

Just east of this bend, the N–S-trending Gagua Ridge is being subducted beneath the Ryukyu Trench along 123°E, as a distinctive re-entrant is observed at where the Gagua Ridge intersects the Yaeyama Ridge (Fig. 1). The Gagua Ridge is an aseismic ridge about 2 km high and 25 km wide, extending from the northeastern corner of Luzon Island to the Ryukyu Trench (Fig. 1). The marine magnetic study of Hilde and Lee (1984) seems to suggest that this ridge is related to a fracture zone. However, the true origin of this ridge is not known yet. Due to its size and continuity, this ridge separates the western-most portion of the Philippine Sea plate, i.e. the Huatung Basin, from the West Philippine Basin. Most of the sediments supplied from the Taiwan mountain belt have been deposited in the Huatung Basin, with the Ryukyu Trench being the only conduit for transporting the sediments across this ridge to the east, resulting in a bathymetric difference of about 1000 m between the West Philippine Basin and the Huatung Basin.

Three multi-channel seismic reflection profiles collected during the TAICRUST survey in the south Ryukyu margin provide details of the forearc deformation caused by the subducted Gagua Ridge. In this paper, we present the analyses of these three seismic profiles which are located to the east, west, and north of the Gagua Ridge, respectively (Fig. 1). Structural features which correspond to different stages of the ridge subduction are also discussed.

2. Data acquisition and processing

The deep seismic reflection data were collected by the R/V *Maurice Ewing* (cruise EW9509) during the TAICRUST survey in August and September of 1995. The TAICRUST project is a seismic imaging program that utilizes deep seismic reflection profiles and wide-angle reflection and refraction data (recorded by both ocean bottom seismometers and onland seismic stations) to investigate the deep structure and geodynamic processes of the south Ryukyu margin and the Taiwan arc–continent collision zone (Liu et al., 1995). The seismic source used was a 20-airgun array with a total volume of 8420 in^3 fired at 20-s intervals. 16 s of seismic reflection data received by a 160-channel digital streamer 4000 m in length were recorded. This data set was processed using both SIOSEIS and ProMAX seismic processing software on two SUN SPARC20 workstations at the Institute of Oceanography, National Taiwan University.

Navigation was provided by differential GPS, using data recorded simultaneous onboard the R/V *Maurice Ewing* and at the base station at the National Taiwan University, respectively, to obtain the most accurate ship positioning data. Shot locations where further smoothed over a 10-min time gate and seismic geometry was assigned based on a 12.5 m common-mid-point (CMP) interval. Special efforts have been made to derive the best velocity information from the seismic reflection data. Along each profile, stacking velocities were interactively analyzed at every 100th CMP based on maximum semblance of a 6-CMP super-gather. These velocity picks were then interpolated along the sea floor to a regular velocity grid with a spacing of 20 CMPs and 48 ms. Horizon velocity analyses were performed in order to optimize the stacking velocity field. Based on the stacking velocity field, true amplitude recovery was applied to correct for spherical divergence attenuation. Then, Q compensation was derived from the interval velocity field and applied to correct for inelastic frequency-dependent attenuation. Frequency analysis revealed a frequency content centered around 40 Hz with −25 dB offset below 4 Hz and above 70 Hz. A minimum phase Ormsby band pass filter with corner frequencies of 3–8–60–70 Hz was applied. No multiple attenuation is applied in the sections presented in this study.

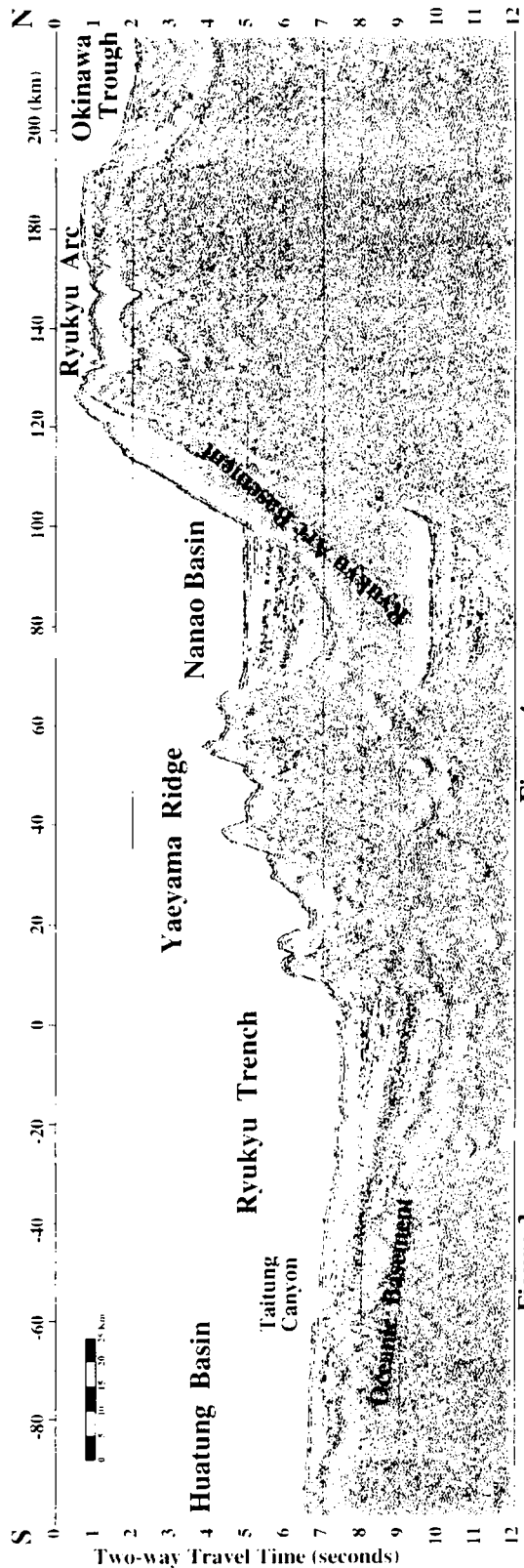

Fig. 2. Time-migrated seismic section of profile 1 (line EW9509-1). This profile runs north–south (see Fig. 1 for location) across the Okinawa Trough, the Ryukyu Arc, the Nanao forearc basin, the Yaeyama accretionary ridge, the Ryukyu Trench, and ends in the Huatung Basin (see Fig. 1 for location). Vertical exaggeration at sea floor is about ×10. Sections of the profile that are shown in Figs. 3 and 4 are marked by arrows below the profile.

A model-based transform (Naess, 1992) was used to weight CMP gathers and a final stack was produced. Finally, a migration velocity field was constructed based on 85% to 75% of the interval velocities derived from the stacking velocities, and further filtered between 1480 m/s and 4000 m/s. Fast explicit finite-difference post-stack time migration (Soubaras, 1992) was performed to generate final seismic sections.

Three seismic profiles are analyzed in this study. Profile 1 (line EW9509-1) consists of 9422 shots with an average shot spacing of 34 m and a total length of 325 km (Fig. 2). This profile is located west of the Gagua Ridge and is roughly perpendicular to the Ryukyu Trench. Only the portion south of the Ryukyu Arc is discussed in this study (Figs. 3 and 4). Profile 2 (line EW9509-18) consists of 2875 shots with an average shot spacing of 53 m and a total length of 153 km. Parallel to profile 1, it is located east of the Gagua Ridge (Fig. 5). Profile 3 (line EW9509-14) consists of 4978 shots with an average shot spacing of 37 m and a total length of 186 km. It runs parallel to the Ryukyu Trench along the axis of the forearc basin. In this study, we present only the eastern half of the profile (Fig. 6) where the forearc basin structure is affected by the subducting Gagua Ridge.

3. Seismic interpretation

3.1. The Philippine Sea plate

In the southern portion of profiles 1 and 2 (Figs. 3 and 5, respectively), the Philippine Sea oceanic crust is covered by a thin layer (<1 s TWT) of sediments. The thickness of the sediments increases progressively northward to 2.7 s TWT at the trench axis. The top of the oceanic crust on both sides of the Gagua Ridge lowers from 7 s TWT at the outer rise to 10 s TWT at the trench axis. A submarine canyon, the Taitung Canyon, cuts across the southern portion of profile 1 (Fig. 3). It appears to be located above a fracture within the oceanic plate where a one-second offset in the oceanic basement is observed. A second canyon, the Hualien Canyon, intersects this profile near the trench axis. The thick trench fills are mainly derived from the Taiwan mountain belt and transported here by these two major submarine canyons.

The submarine canyons are not well expressed east of the Gagua Ridge. East of the Gagua Ridge (around 123°30′E), several volcanoes rise from the sea floor in the West Philippine Basin. Profile 2 runs across one of such cylindrical volcanoes (between −28 and −38 km in Fig. 5).

A sub-basement reflection is observed on profile 1 at about 1.5 s TWT below the top of the oceanic basement, between −68 and −45 km, as a high-amplitude long-wavelength reflector (Fig. 3). A similar reflector is imaged on profile 2 between −25 and 0 km (Fig. 5). This sub-basement reflection could be Moho. However, if it is Moho, due to the small time interval (<1.5 s TWT) between the basement reflection and this sub-basement reflection, the igneous oceanic crust would be very thin (less than 5 km), and even thinner towards the trench. Previously conducted seismic refraction surveys offshore south Ryukyu (Murauchi et al., 1968) and north Ryukyu (Ludwig et al., 1973; Iwasaki et al., 1990) show a strong velocity contrast between layer 2 and layer 3 (5600–7000 m/s) and an abnormally thin layer 3. Therefore, the continuous sub-basement reflector imaged on our seismic profiles could represent the top of the oceanic layer 3, whereas the Moho, which should lie less than 1 s TWT deeper, is not well imaged. Further south, this sub-basement reflection is less clearly imaged but provides a realistic crustal thickness of about 7 km. Crustal velocity structures derived from ocean bottom seismometer data collected along profile 1 (Wang et al., 1996) may provide a better constraint on the interpretation of this sub-basement reflection.

3.2. The Ryukyu Trench and Yaeyama Ridge

The Ryukyu Trench, at a roughly constant water depth of 6000 m, is tortuous in the study area. The Yaeyama Ridge is about 50 km wide, with depths ranging from 6000 m to 3000 m. It is formed by an imbricated and folded wedge of sediments.

Along profile 1 (Fig. 4), the topography of the Yaeyama Ridge is characterized by ridges, domes and troughs. It is difficult to recognize the precise location of the décollement on this seismic section. However, it appears that most of the terrigenous sediments entering the subduction zone are frontally accreted. The top of the subducting Philip-

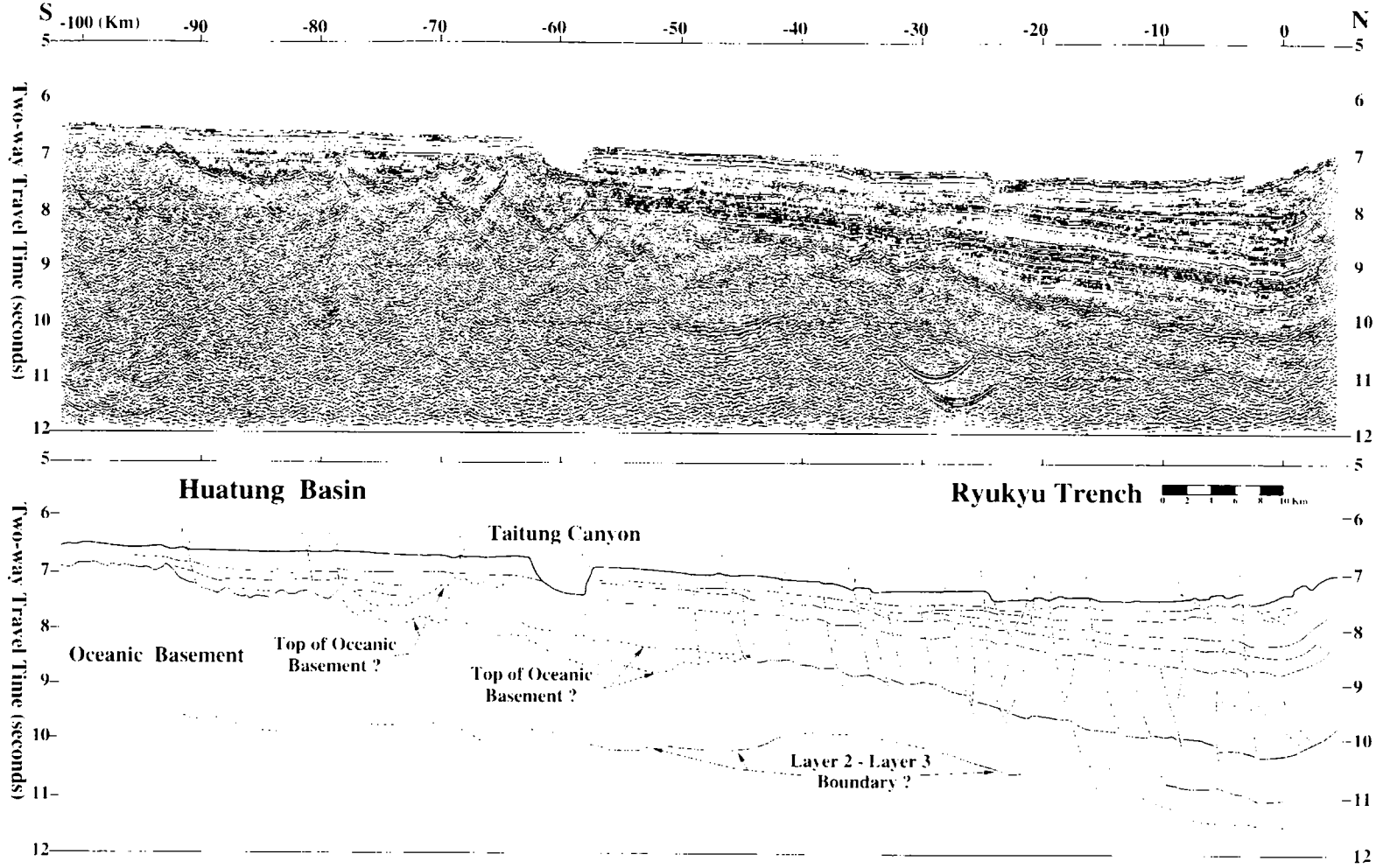

Fig. 3. Seismic image of the Huatung Basin and Ryukyu Trench from profile 1 (upper figure) and its structural interpretation (lower figure). Vertical exaggeration at sea floor is about ×6.2.

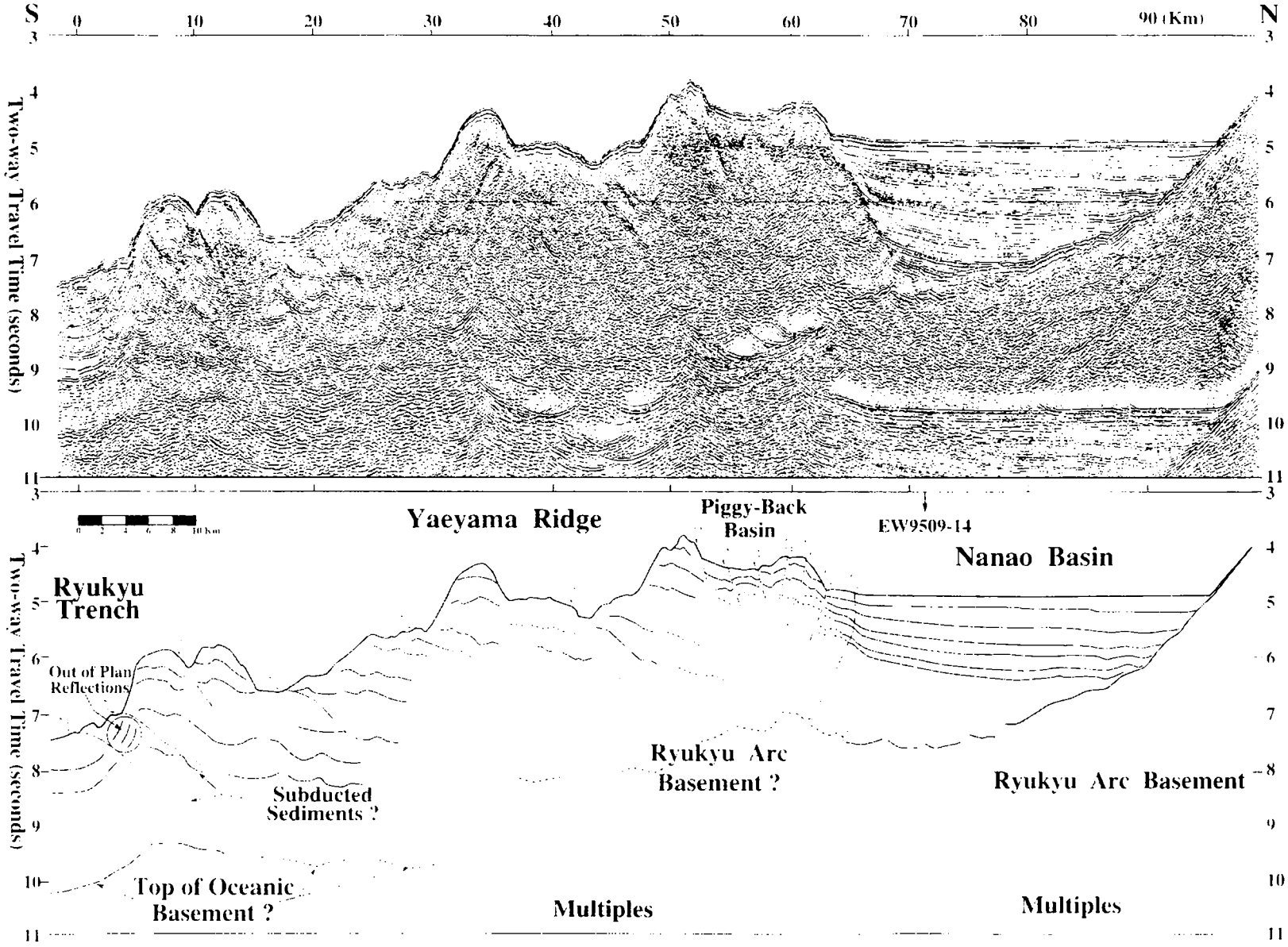

Fig. 4. Seismic image of the Yaeyama Ridge and Nanao Basin from profile 1 (upper figure) and its structural interpretation (lower figure). Vertical exaggeration at sea floor is about ×6.2.

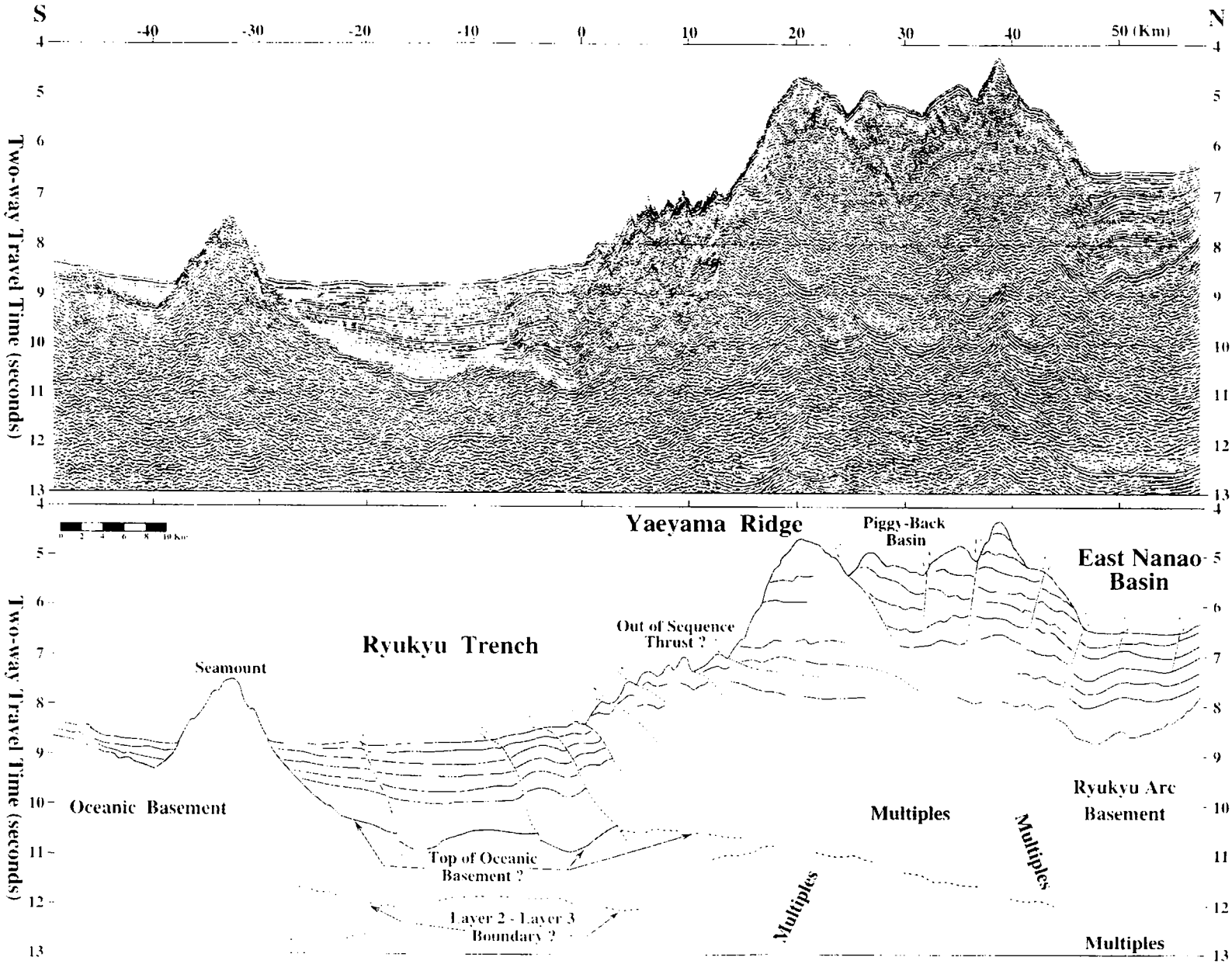

Fig. 5. Seismic image of the Ryukyu Trench and Yaeyama Ridge along profile 2 (upper figure) and its structural interpretation (lower figure). See Fig. 1 for profile location. Vertical exaggeration at sea floor is about ×6.2.

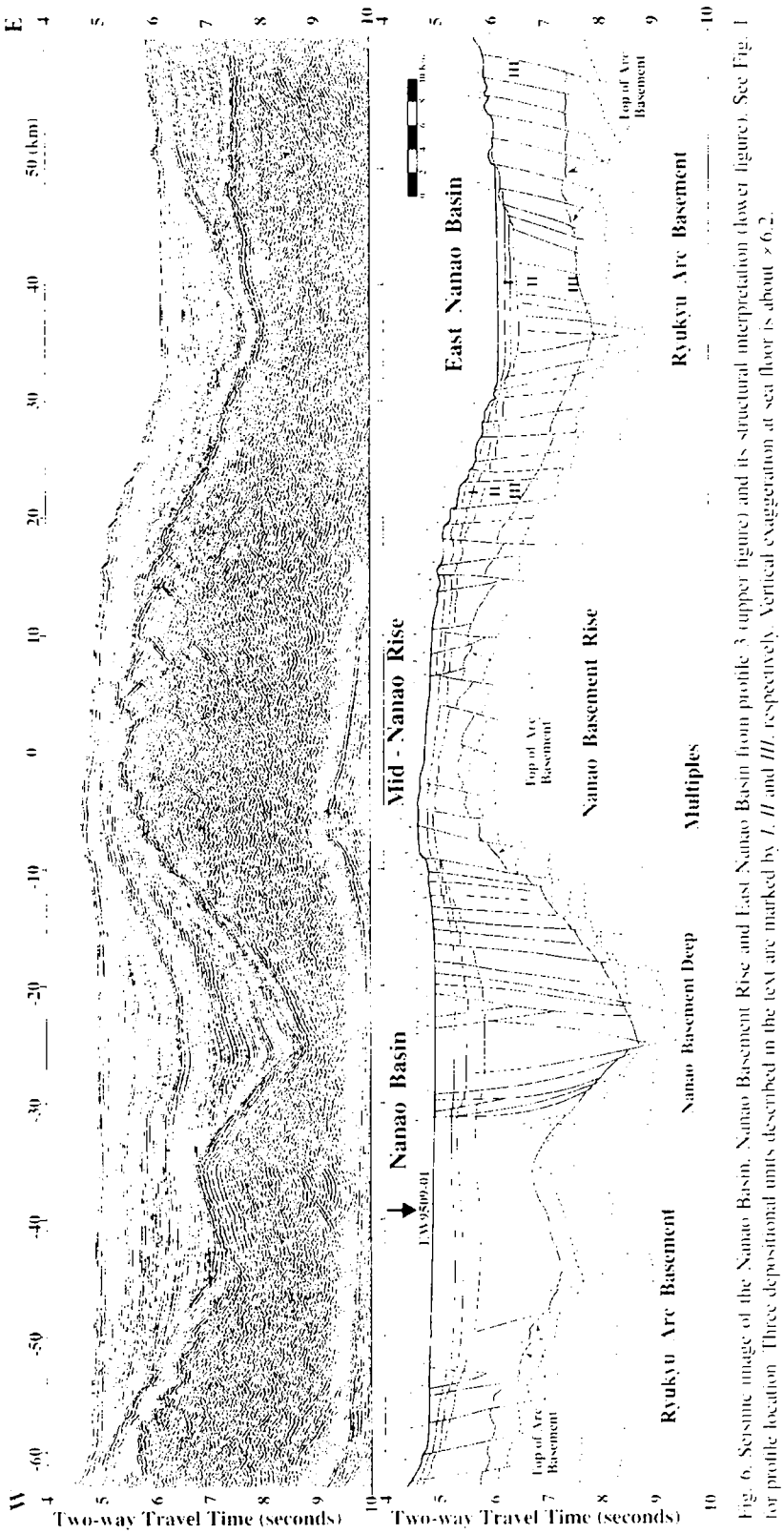

Fig. 6. Seismic image of the Nanao Basin, Nanao Basement Rise and East Nanao Basin from profile 3 (upper figure) and its structural interpretation (lower figure). See Fig. 1 for profile location. Three depositional units described in the text are marked by *I*, *II* and *III*, respectively. Vertical exaggeration at sea floor is about ×6.2.

pine Sea plate can be traced at depths of 9.5 to 10 s TWT beneath the toe of the Yaeyama Ridge to about 35 km from the trench axis, then it is masked by the water-bottom multiple. The toe of the overriding accretionary wedge is cut by many thrust faults while back-thrust faults were developed in the northern portion of the accretionary wedge. A piggy-back basin lies between the frontal thrusts and back-thrusts near the northern edge of the Yaeyama Ridge (Fig. 4).

Along profile 2 (Fig. 5), the topography of the Yaeyama Ridge is characterized by a sudden break of the trench slope from 2 to 10 degrees. A major out-of-sequence thrust probably outcrops at the base of the steep slope. The sediments south of this out-of-sequence thrust are poorly imaged. Again, most of the sediments entering the trench seem to be frontally accreted. The top of the subducting Philippine Sea plate can be traced at depths of 9.5 to 10 s TWT beneath the toe of the Yaeyama Ridge to 20 km from the trench axis, then less clearly at 11–11.5 s TWT to 40 km. Similar to profile 1, back-thrusts may affect the northern edge of the Yaeyama Ridge.

3.3. *The forearc basin*

Between the Yaeyama Ridge and the Ryukyu arc lies a forearc basin 30–35 km wide (Fig. 1). On the southern side, the forearc basin sediments were trapped against the rear of the Yaeyama Ridge where the development of back-thrusts has progressively thickened the accretionary wedge (Figs. 4 and 5). On the northern side, the forearc basin is bounded by the southern flank of the Ryukyu Arc (Fig. 4). The depth of the forearc basin here is about 3600 m. Within a horizontal distance of only 26 km, the sea floor ascends to about 1000 m where it reaches the shelf of the Ryukyu Arc (Fig. 2). This slope should be the southern boundary of the Paleozoic–Mesozoic basement of the non-volcanic Ryukyu Arc that formed a back-stop against which the Yaeyama accretionary complex is built. Few coherent reflections are imaged within the arc basement.

Profile 3 runs roughly east–west along the axis of the forearc basin. A basement high in the forearc basin, aligned with the northward projection of the subducting Gagua Ridge, divides the forearc basin into the Nanao Basin and the East Nanao Basin (Fig. 6). Profile 1 crosses the Nanao Basin near its center (~38 km in Fig. 6), whereas profile 2 surveys the eastern edge of the East Nanao Basin.

The Nanao Basin is about 75 km long. Its maximum sediment thickness is about 4 s TWT (Fig. 6). In the western half of the Nanao Basin, sediments are almost undeformed with continuous parallel reflections lying unconformably on the forearc basement. The basement shows a double stepwise arrangement: the basement depth drops from 5.7 to 7.2 s TWT in the western part of the Nanao Basin, then deepens again from 7 to 9.2 s TWT near the center of the Nanao Basin where the basement reaches its deepest point (called the Nanao Basement Deep). Several conjugate normal faults cut the entire sedimentary sequences down to the Nanao Basement Deep. East of the depocenter, the basement rises to form a structural high (called the Nanao Basement Rise) which separates the Nanao Basin from the East Nanao Basin. Sediments are lying conformably on top of the basement. Numerous westward-dipping normal faults cut both the Nanao Basin strata and the forearc basement.

The Nanao Basement Rise is composed of east-dipping tilted blocks covered by 0.7 s TWT of recent sediments (Fig. 6). However, few coherent reflectors are imaged within the basement rise and its precise structure is difficult to see. Eastward, the basement progressively deepens into the East Nanao Basement Deep located in the center of the East Nanao Basin.

Unlike the Nanao Basin which consists of mainly turbidites from the Taiwan mountain belt, the East Nanao Basin shows a more complicated depositional history. Three different depositional units can be recognized (Fig. 6). The oldest unit (unit III), lying on top of the forearc basement, consists of a series of west-dipping layers that thins from 1.2 s TWT at the eastern end of the profile to 0.5 s TWT in the center of the East Nanao Basin, then progressively vanishes toward the west. Above this depositional unit lies a sequence of sediments (unit II) with a similar seismic signature as the Nanao Basin turbidites. In the eastern part of the basin, this sequence is relatively flat and cut by several normal faults of small cumulative throw. Its thickness reaches 1.5 s TWT in the center of the East Nanao Basin. Further to the west, this unit is tilted towards the east and cut by numer-

ous east-dipping normal faults as they slide down the Nanao basement rise. The most recent sedimentary unit (unit I) is flat and undeformed.

4. Discussion

Topographically, the Gagua Ridge appears to end in the Ryukyu Trench. However, a re-entrant of 18.5 km (20 km wide) attests that a portion of the Gagua Ridge has already been subducted. Newly acquired seismic data confirm that the Gagua Ridge does extend continuously northward underneath the thick trench fill (Char-Shine Liu, unpublished seismic data, 1997). In the study area, the Ryukyu Trench axis is oriented between N270° and N280° while the relative convergence rate between the Philippine Sea and Eurasia plates is about 7.1 cm/yr in a direction of N308°. Given the high obliquity (>50°) of the plate convergence here, the subducted portion of the Gagua Ridge should have progressively crept northwestward under the Yaeyama Ridge east of 123°E. Ridge subduction has been extensively documented in the literature (e.g. Fryer and Smoot, 1985; Lonsdale, 1986; Lallemand and Le Pichon, 1987; Collot and Fisher, 1989; Lallemand et al., 1990; Von Huene and Scholl, 1991). Lallemand et al. (1994) described the processes related to subduction of an asperity in the following four stages (Fig. 7).

(a) Initial stage. The overriding plate is assumed to behave as a non-cohesive Coulomb wedge which slides frictionally over a rigid base (the subducting plate). This wedge obeys the critical taper model derived by Davis et al. (1983) and Dahlen (1984).

(b) Indentation of the margin. The subduction of

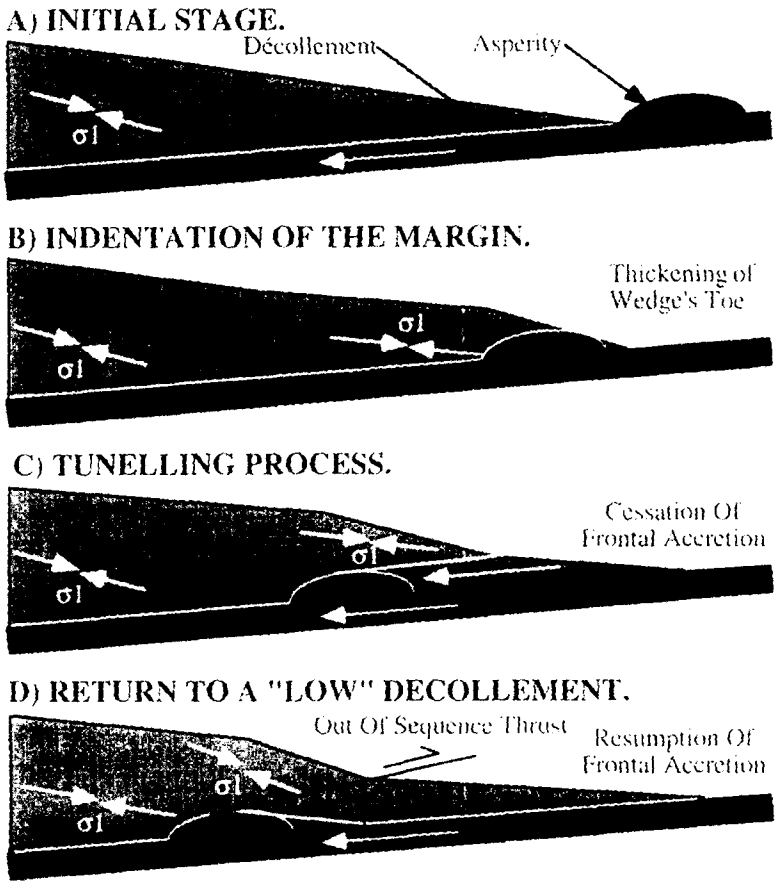

Fig. 7. Evolution of an asperity subduction. Four stages are shown in cross-sections to reveal a short-lived sequence of indentation, tunneling and resumption of frontal accretion as the asperity is subducted (after Lallemand et al., 1994).

the asperity under the accretionary wedge forces the décollement to move up above the asperity. Thickening of the prism occurs above the landward flank of the asperity. The high friction along this newly formed décollement develops a steep frontal slope above the trailing flank of the asperity.

(c) Tunneling process. While the décollement is forced in this 'shallow' position, frontal accretion of the incoming sediments ceases. Those sediments, in the wake of the indentor, are thus easily subducted (Ballance et al., 1989) beneath the newly formed décollement and its overlying wedge, leaving a re-entrant in the deformation front.

(d) Return to a mechanically least resistant 'basal' décollement. After a certain amount of penetration of the asperity, the décollement jumps down to the vicinity of its initial position, restoring a level of minimum resistance. The older 'shallow' décollement is fossilized in the form of an out-of-sequence thrust. Frontal accretion then resumes.

The observed structural differences between profile 1 and profile 2 thus can be clarified. The overall shape of the Yaeyama Ridge is a typical accretionary wedge built by imbrication of frontal units during the subduction process. The internal structures along profile 1 consist of seaward-verging anticlinal ridges bounded by arcward-dipping thrusts that express the accretionary nature of the lower slope. In the northern extension of the Gagua Ridge, the re-entrant in the Ryukyu Trench and the thickened Yaeyama Ridge, as observed on the bathymetric map (Fig. 1), are characteristic of the cessation of frontal accretion as the décollement migrates upward above the subducted portion of the ridge. The sudden change in the steepness of the lower trench slope along profile 2, between 13 and 20 km from the trench, marks the outcrop of the elevated décollement. However, frontal accretion within the incoming sediments appears to have resumed on this seismic profile, attesting to the fact that the décollement has returned to a basal position. The shallow arcward-dipping out-of-sequence thrust which crops out at the base of the cliff can thus be interpreted as the past activity of a 'high' décollement inherited above the subducting ridge. The newly accreted units are underthrust beneath the out-of-sequence thrust. The arcward extension of this thrust is unclear on the seismic section.

The basement high separating the Nanao Basin from the East Nanao Basin is aligned with the northward projection of the Gagua Ridge (Fig. 1). We suggest that the rise of the basement imaged across the axis of the forearc basins is caused by the subducted Gagua Ridge. The onlap pattern of the sediments deposited on the western flank of the Nanao Rise suggests that the uplift is syn-sedimentary. The divergent depositional pattern as well as the offsets along the west-dipping normal faults suggest a steady basement uplift occurring mainly in the later stage of the basin infill. The western part of the Nanao Rise is still actively uplifting.

On the eastern flank of the Nanao Rise, the normal faults have affected both the forearc basement and the overlying eastward tilted sediments. This suggests that the subsidence occurred following the uplift. In the East Nanao Basin, the most recent sediments (unit 1) are undisturbed, indicating that this area is now back to a stable situation. These observations fit very well with the hypothesis that the arc basement was uplifted by the obliquely subducted Gagua Ridge underneath.

Finally, the high obliquity of the plate convergence may result in strain partitioning within the overriding plate (e.g. Fitch, 1972). Strike-slip fault preferentially occurs along the contact between the accretionary wedge and the consolidated back-stop (the arc basement), as has been described along the Mentawai Fault off Sumatra (Diament et al., 1992). The trenchward extension of the arc basement, clearly imaged underneath the Nanao Basin, is not well constrained under the accretionary wedge on our seismic profiles. The back-thrusts affecting the northern edge of the Yaeyama Ridge might provide a natural slip plane for a high-angle shear zone (Figs. 4 and 5).

Furthermore, we can see from Fig. 1 that the East Nanao, Nanao, and Hoping forearc basins lie with stepwise northwestward offsets, correlating to the kinks in the bathymetric contours along the southern flank of the Ryukyu Arc. The opening of the Okinawa Trough back-arc system might be responsible for this southward stepwise pattern of the southern flank of the Ryukyu Arc (Hsu et al., 1996). These observations may also imply that a much wider part of the Ryukyu margin accommodates the oblique subduction.

5. Conclusions

Multi-channel seismic reflection profiles and bathymetric data in the south Ryukyu margin reveal the complicated nature of the forearc structures where the Gagua Ridge is being subducted obliquely beneath the Yaeyama Ridge. The prominent re-entrant developed at the toe of the Yaeyama Ridge where the Gagua Ridge enters the Ryukyu Trench, shows that the indentation process is active at the present time. The analyses of two N–S-trending seismic profiles located on either side of the Gagua Ridge suggest that the out-of-sequence thrust observed in the frontal portion of the Yaeyama Ridge on the seismic section to the east of the Gagua Ridge might be formed due to the passage of the Gagua Ridge underneath the accretionary wedge following the northwesterly direction of plate convergence. The uplift of the forearc basement which separates the Nanao and East Nanao basins to the north of the re-entrant, together with the depositional and structural patterns of the forearc basin strata, suggest that at least a 100 km section of the Gagua Ridge has been subducted, and the ridge has kept its north south-trending configuration underneath the forearc region of the south Ryukyu margin.

Due to the high obliquity of the plate convergence in the south Ryukyu margin, strain partitioning within the frontal portion of the Ryukyu margin may well be superimposed onto the ridge subduction. In the accretionary wedge, the ridge subduction is likely to have a dominant control. Further north, as the Gagua Ridge gets deeply buried (as its depth becomes large compared to its height), regional tectonic forces, such as the Taiwan arc–continent collision occurring just to the west of the study area and the opening of the Okinawa Trough back-arc basin, should all be taken into account when examining the structures of the south Ryukyu margin.

Acknowledgements

We would like to thank both the crew and technical personnel of the R/V *Maurice Ewing*, cruise EW9509, for their efforts in acquiring these excellent data despite the visits of five typhoons. G.F. Moore helped a great deal in showing us how to use the ProMAX seismic data processing system. Discussion with G.F. Moore and N. Lundberg during the EW9509 cruise and with J. Malavieille, J. Angelier, M. Fournier and S. Dominguez during the ACT cruise have improved our understanding of the regional tectonic structures. J.-C. Sibuet and S.-K. Hsu provided indispensable information on the opening of the Okinawa Trough. S.-Y. Liu has compiled the bathymetric maps used in this paper. Comments made by E. Flueh, W. Mooney and an anonymous reviewer have improved the quality of this paper. This study presents part of the results of the TAICRUST project jointly funded by the National Science Council, R.O.C. (grants NSC83-0209-M-002A-031Y, NSC83-0501-I-002-057-B42 and NSC84-0209-M-002A-001Y to C.-S. Liu) and the National Science Foundation, U.S.A. (grant OCE94-16583 to D. Reed, N. Lundberg and G.F. Moore).

References

Ballance, P.F., Sholl, D.W., Vallier, T.L., Stevenson, A.J., Ryan, H., Herzer, R.H., 1989. Subduction of a late Cretaceous seamount of the Louisville Ridge at the Tonga Trench: a model of normal and accelerated tectonic erosion. Tectonics 8 (5), 953–962.

Collot, J.-Y., Fisher, M.A., 1989. Formation of the forearc basins by collision between seamounts and accretionary wedges: an example from the new Hebrides island arc. Geology 17, 930–934.

Dahlen, F.A., 1984. Mechanics of fold and thrust belts and accretionary wedges: cohesive Coulomb theory. J. Geophys. Res. 89, 10087–10101.

Davis, D., Suppe, J., Dahlen, F.A., 1983. Mechanics of fold and thrust belts and accretionary wedges. J. Geophys. Res. 88, 1153–1172.

Diament, M., Harjono, H., Karta, K., Deplus, C., Dahrin, D., Zen, M.T., Gerard, M., Lassal, O., Martin, A., Malod, J., 1992. Mentawai fault zone off sumatra: a new key to the geodynamics of western Indonesia. Geology 20, 259–262.

Fitch, T.J., 1972. Plate convergence, transcurrent faults, and internal deformation adjacent to southeast asia and western Pacific. J. Geophys. Res. 77 (23), 4432–4460.

Fryer, P., Smoot, N.C., 1985. Processes of seamount subduction in the Mariana and Izu-Bonin Trenches. Mar. Geol. 64, 77–90.

Hilde, T., Lee, C.-S., 1984. Origin and evolution of the West Philippine Basin: a new interpretation. Tectonophysics 102, 85–104.

Ho, C.-S., 1986. A synthesis of the geological evolution of Taiwan. Tectonophysics 125, 1–16.

Hsu, S.-K., Sibuet, J.-C., Monti, S., Shyu, C.-T., Liu, C.-S., 1996. Transition between the Okinawa Trough backarc extension and the Taiwan collision: new insights on the southernmost

Ryukyu subduction zone. Mar. Geophys. Res. 18, 163–187.
Iwasaki, T., Hirata, N., Kanazawa, T., Melles, J., Suyehiro, K., Urabe, T., Möller, L., Makris, J., Shimamura, H., 1990. Crustal and upper mantle structure in the Ryukyu Island Arc deduced from deep seismic sounding. Geophys. J. Int. 102, 631–651.
Kizaki, K., 1986. Geology and tectonics of the Ryukyu Islands. Tectonophysics 125, 193–207.
Lallemand, S.E., Le Pichon, X., 1987. Coulomb wedge model applied to the subduction of seamounts in the Japan Trench. Geology 15, 1065–1069.
Lallemand, S.E., von Huene, R., Culotta, R., 1990. Subduction of the Daiichi Kashima seamount in the Japan Trench. Tectonophysics 160, 231–247.
Lallemand, S.E., Schnürle, P., Malavieille, J., 1994. Coulomb theory applied to accretionary and non-accretionary wedges: possible causes for tectonic erosion and or frontal accretion. J. Geophys. Res. 99 (B6), 12033–12055.
Lallemand, S.E., Liu, C.-S., Font, Y., 1997. A tear fault boundary between the Taiwan orogen and the Ryukyu subduction zone. Tectonophysics 274, 171–190.
Le Pichon, X., Huchon, P., Barrier, E., 1985. Geoide and evolution of the western margin of the Pacific Ocean. In: Nasu, N. (Ed.), Formation of Active Margins. Terra Publ., Tokyo, pp. 3–42.
Liu, C.-S., Reed, D.L., Lundberg, N., Moore, G.F., McIntosh, K.D., Nakamura, Y., Wang, T.K., Chen, T.H., Lallemand, S., 1995. Deep seismic imaging of the Taiwan arc–continent collision zone. EOS, Trans. Am. Geophys. Union 76 (46), F635.
Liu, C.-S., Lallemand, S.E., Lin, S.-J., 1996a. Structural characteristics and possible boundary between the Taiwan collision zone and the Ryukyu arc-trench system. In: Proceedings of the Geological Symposium in Memory of Prof. T.-P. Yen. National Central University, Chung-Li, Taiwan, pp. 267–275.
Liu, C.-S., Liu, S.-Y., Song, G.-S., Shyu, C.-T., Yu, H.-S., Chiao, L.-Y., Wang, C.-S., Karp, B., 1996b. Digital bathymetry data offshore Taiwan. 1996 Annu. Meet. Geol. Soc. China, Prog. Abstr., pp. 420–425.
Lonsdale, P.F., 1986. A multibeam reconnaissance of Tonga Trench axis and its intersection with the Louisville Guyot Chain. Mar. Geophys. Res. 8, 295–327.
Ludwig, W., Murauchi, S., Den, N., Bull, P., Hotta, H., Ewing, M., Asanuma, T., Yoshii, T., Sakajiri, N., 1973. Structure of east China Sea–West Philippine margin off southern Kyushu, Japan. J. Geophys. Res. 78, 2526–2536.
Murauchi, S., Den, N., Asana, S., Hotta, H., Yoshii, T., Asanuma, T., Hagiwara, K., Sato, T., Ludwig, W.J., Ewing, J.I., Edgar, N.T., Houtz, R.E., 1968. Crustal structure of the Philippine Sea. J. Geophys. Res. 73, 3143–3171.
Naess, O.E., 1992. Application of modelbased transformations for seismic interpretational analysis. First Break 10, 313–322.
Seno, T., Stein, S., Gripp, A.E., 1993. A model for the motion of the Philippine Sea Plate with NUVEL-1 and geological data. J. Geophys. Res. 98, 17941–17948.
Soubaras, R., 1992. Explicit 3D migration using equiripple polynomial expansion and Laplacian synthesis. SEG Annu. Meet. Expanded Abstr., pp. 905–908.
Teng, L.-S., 1990. Geotectonic evolution of the late Cenozoic arc-continent collision in Taiwan. Tectonophysics 183, 57–76.
Von Huene, R., Scholl, D.W., 1991. Observations at convergent margins concerning sediment subduction, subduction erosion, and the growth of continental crust. Rev. Geophys. 29, 279–316.
Wang, T.-K., McIntosh, K., Nakamura, Y., Liu, C.-S., 1996. OBS refraction survey and imaging offshore eastern Taiwan. EOS, Trans. Am. Geophys. Union 77 (46), F720.
Wessel, P., Smith, W.H.F., 1995. The Generic Mapping Tool (GMT) version 3.0. Technical Reference and Cookbook. SOEST/NOAA.